Arab J. Nucl. Sci. Appl., Vol. 58, 2, 29-43 (2025)

ISSN 1110-0451

Arab Journal of Nuclear Sciences and Applications

Web site: ajnsa.journals.ekb.eg

(E S N S A)

Breast Cancer Suppression by Radiation Prepared Nanoformulation of Se@Pt-AG-FA NPs through Apoptotic Pathway

Alyaa M. Abd El-Khalek[1], Mohamed K. Abdel-Rafei[1], Mostafa A. Askar[1], Mohamed Salah Soliman[2], Ibrahim Y. Abdelrahman[1*], Nagui Hassan Fares[3]

[(1)]Radiation Biology Research Department, National Centre for Radiation Research and Technology (NCRRT), Egyptian Atomic Energy Authority (EAEA), Cairo, Egypt

[(2)]Radiation Research of Polymer Chemistry Department, Industrial Irradiation Division, National Centre for Radiation Research and Technology (NCRRT), Egyptian Atomic Energy Authority (EAEA), Cairo, Egypt

[(3)]Department of Zoology, Faculty of Science, Ain Shams University, Cairo, Egypt.

ARTICLE INFO

Article history:

Received: 11th Dec. 2024

Accepted: 2nd Feb. 2025

Available online: 1st Mar. 2025

Keywords:

Breast Cancer;
Nanoparticles;
Targeting therapy;
Selenium;
Pterostilbene.

ABSTRACT

Breast cancer is the most fatal malignancy in females. Among various cancer therapies, targeted therapy focuses on specific factors in cancer cells to slow tumor growth without damaging healthy cells. Se NPs are promising anticancer agents and can be enhanced by conjugating targeting molecules like Folic Acid and Pterostilbene loaded on Arabic Gum. Se@Pt-AG-FA nanoformulation was radio-prepared and characterized by TEM. The experimental design involved: 60 female rats divided into three groups: negative control (n=10), positive control (n=20), and treated group (n=20) with an intraperitoneal injection of Se@Pt-AG-FA (4ml/kg/twice weekly for 2 months), the last two groups bearing breast cancer induced by MNU. The tumor volume and survival rate were recorded weekly. In breast tissues, the gene expressions of *BCL2* and *BAX* were evaluated by RT-PCR, and a pathological examination was done. Also, CBC parameters were assessed. The current results recorded that Se@Pt-AG-FA reduced the tumor volume to 9.98 mm^3 and increased the survival rate to 75% in the treated group. Se@Pt-AG-FA upregulates *BAX* gene expression (17.2) and downregulates *BCL2* gene expression (0.196), and the *BAX/BCL2* ratio was recorded at 87.9, an excellent indicator for apoptosis. The pathological examination confirmed that the nanoformulation has a potency effect on breast cancer suppression. In conclusion, Se@Pt-AG-FA has a potent effect as an anticancer targeting therapy for breast cancer models, so it is recommended to increase the validation studies on human cases as a targeting therapy for breast cancer

INTRODUCTION

Breast cancer has become the most fatal malignant tumor in females due to its incidence and drawbacks. The International Agency for Research on Cancer reports that there were about 19 million new cases of breast cancer globally in 2020, with about 10 million deaths related to those cases. [1]. Cancer treatment varies based on tumor type and aggressiveness, including chemo-, radio-, hormone, immune-, and targeted therapies [2]. Targeted therapy focuses on finding chemicals present in cancer cells to slow or stop tumor growth without damaging healthy cells [3]. This therapy targets growth factors, cell membrane receptors, cell cycle mediators, apoptosis regulators, and tumor environment parameters [4]. Nanotechnology, involving tiny molecules ranging from 0.1 to 100 nm, is used in revolutionary methods to improve drug bioavailability, reduce problems and dosage concentration, and deliver drugs to targeted areas with high efficiency [5].

Selenium (Se) is crucial for maintaining body health as a strong antioxidant against reactive nitrogen and oxygen species. It plays a crucial role in the antioxidant system, suppressing the buildup of free radicals in cells. Se can improve the effectiveness of cancer chemotherapy medications due to their anti-oxidative properties [6]. It controls inflammatory enzymes linked

Corresponding author: ebtalah@gmail.com OR Ibrahim.morsy@eaea.org.eg, https://orcid.org/0000-0002-6333-7431
DOI: 10.21608/ajnsa.2025.339343.1866

to carcinogenesis, prevents angiogenesis, inhibits metastasis, and increases the death of malignant cells. Se also inhibits DNA mutation and deactivates transcription factors in cancer cells. Selenium nanoparticles (Se NPs) are emerging as promising anticancer agents due to their bioavailability and lower toxicity compared to selenium compounds. Se NPs' potent anticancer efficacy can be significantly enhanced by conjugating targeting molecules like folic acid arginine-glycine-aspartate (RGD) peptide and transferrin [7].

Pterostilbene (Pt) is an organic substance found in blueberries, grapes, and *Pterocarpus Marsupium*. Its effectiveness is due to its dimethyl ether group, which allows it to pass through cell membranes [8, 9]. Pt has potential in cancer therapy due to its ability to combat inflammation, oxidation, and carcinogenicity. It suppresses the B-cell lymphoma 2 (*BCL2)* and the ERS/ROS pathway, blocks growth factor receptors and reduces DNA damage response [10]. It also works with chemotherapy in breast cancer treatment. Pt is essential for producing reactive oxygen species (ROS) and initiating mitochondrial-mediated apoptosis in breast cancer. It also exhibits anti-inflammatory properties, suppressing inflammatory mediators and reducing endoplasmic reticulum stress-related protein production and cytokine release [11].

Arabic Gum (AG), a biopolymer and proteoglycan found in *Senegal* and *Acacia* trees, is being considered for use in food and pharmaceutical industries due to its safety, coating, emulsification, microencapsulation, and pharmaceutical carrier capabilities [12]. AG's antioxidant properties make it effective in treating diseases, improving immunity, anti-inflammation, and anti-carcinogenesis. It also serves as a stabilizer for Se NPs due to its hydrophilicity, hydroxyl groups, and high surface area [13]. Folic acid (FA), a vital vitamin B found in dark green leafy vegetables and legumes, is crucial for cell metabolism and DNA maintenance [14]. Cancer cells have high levels of folate receptor expression, causing rapid DNA duplication, making it essential for treatment targeting and delivery in breast cancer [15]. Folic acid's high sensitivity, low immune stimulation, and lower molecular weight make it suitable for cancer therapy. Nanoparticles conjugate with specific ligands as folate receptors, enabling precise targeting and low toxicity on normal cells. Targeted therapy targets growth factors, cell membrane receptors, cell cycle mediators, apoptosis regulators, and tumor environment moderators [16].

Apoptosis is a normal process involving gene expression, activation, and regulation, aiming to remove unwanted, abused, and abnormal cells. It plays a crucial role in tissue homeostatic and developmental status, influenced by various factors [17, 18]. Apoptosis aberration in cancer cells leads to mutations, uncontrolled proliferation, differentiation, and angiogenesis, resulting in neoplastic cells and tumor development [14, 19]. Cancer cells evade apoptosis through anti-apoptotic modulators, suppression of pro-apoptotic signals, defective pathways, and impaired functions, making them resistant to chemotherapy. Deactivation of pro-apoptotic factors is evident in breast, small-cell lung, and gastric cancer. The *BCL2* protein family is a group of key regulators with pro- and anti-apoptotic activities. They can either cause cells to die irreversibly or allow them to escape apoptosis and become malignant [20]. The *BCL2* family is divided into three subgroups: anti-apoptotic/pro-survival proteins such as *BCL2*, pro-apoptotic proteins such as *BCL2*–associated X protein (*BAX)*, and pro-apoptotic BH3-only proteins. The *BAX* to *BCL2* expression ratio is a crucial cell death switch, determining cell life or death in response to apoptotic stimuli. An increased ratio reduces cellular resistance, increasing cell death and reducing tumor incidence [21]. Nanoparticles offer enhanced precision, control, and versatility in cancer therapy, leading to more effective treatments compared to traditional natural products due to their ability to targeted delivery, controlled release, enhanced bioavailability, multifunctionality, small size, and penetration. Therefore, this study aims to investigate the antitumor effects of the new formulation Se@Pt-AG-FA NPs which is synthesized by radiation through apoptotic pathway.

MATERIALS AND METHODS

1. Materials

1.1. Chemicals

Pt was purchased from Sigma Aldrich, MDL Number: MFCD00238710. Sodium Selenite (Anhydrous) 98% was purchased from Loba Chemie. FA was purchased from Qualikems® (India). AG from acacia tree was purchased from Sigma-Aldrish, MDL Number: MFCD00081264. 1-methyl-1-nitrosourea (MNU) was purchased from Toronto Research Chemicals Inc., Canada, Cat#M325815 Lot#14-RCD-53-3. Thiopental Sodium was purchased from Egyptian INT. Pharmaceutical Industries CO., Egypt. Saline was purchased from EL-NASR Pharmaceutical Chemicals Co. Egypt.

1.2. Experimental animals

The study involved 60 female *Sprague-Dawly* rats aged 28 days, placed in the animal breeding unit for five days to acclimate and adapt. In addition, they were divided into five rats each plastic cage, and kept in a room with ideal circumstances, such as enough ventilation, a temperature of 25 °C, a 12-hour light/dark cycle, and a humidity level between 60 and 70%.

The animals were obtained from the National Centre for Radiation Research and Technology (NCRRT), Animal Breeding Unit, Egyptian Atomic Energy Authority (EAEA), Cairo, Egypt. The rats were divided into 10 rats as negative control and 50 for tumor induction groups, and placed in optimum conditions. Breast cancer was induced using MNU prepared by dissolving it in 0.9% NaCl and acetic acid. The induction was done *in situ* with 50 mg/kg doses at ages 33, 40, 47, 54, and 61 days [22]. The rats were left for tumor growth for two months after the last injection, and palpations were performed weekly to estimate the progress of the masses. After two months, 40 rats that had a tumor mass were selected, while 6 female rats died during induction and 4 rats were excluded due to the outer layer of their tumor volume than other animals bearing breast cancer masses.

1.3. Experimental design

The experiment involved 10 normal rats as negative control group that just received an intraperitoneal saline injection, 20 breast cancer-bearing rats induced by MNU as the positive control group that also just received saline injection intraperitoneally, and 20 breast cancer-bearing rats for treated group that given Se@Pt-AG-FA NPs twice a week for two months, at a dosage of 4 ml/kg of body weight in each rat (0.6 ml for each weighting 150 gm).

1.4. The ethical committee approval

The experimental design for animal usage was approved through the Ethical committee at the National Centre for Radiation Research and Technology with code number 47A/22.

2. Methods

2.1. Preparation of nanoformulation

The process involved dissolving AG in distilled water overnight and adding FA, sodium selenite, and Pt in DMSO (0.5%). The final solution was sonicated for 30 minutes and exposed to gamma radiation at 2.5 kGy. The stock solution of the prepared drug contained 1% AG, 1% FA, 1% sodium selenite, and 2% Pt in a 100 ml volume.

2.2. Nanoformulation characterization

TEM images were captured using a transmission electron microscope (TEM), model JEM1010 (JEOL, Japan). The size and size distribution of the SeNPs were determined.

2.3. Survival Curve

Using the Kaplan-Meier method, survival analysis was performed.

2.4. Tumor volume

Tumor volume is a crucial method for monitoring tumor progression. A ruler was used to measure the dimensions of solid tumors in both the positive control and the treated groups. The tumor volume of a solid tumor was calculated using the formula $V= (W^2 L)/2$, where V is the tumor volume, W is the tumor width, and L is the tumor length [23]. The average tumor volume in the positive control and treated group at the beginning of the treatment protocol were 68.67 mm^3 and 71.42 mm^3, respectively with no significant difference (*P*-value = 0.77).

2.5. Sampling

At the end of the experiment, the animals were injected intraperitoneally with Thiopental (50mg/kg) and Atropine (50µg/Kg) [24]. The blood samples were taken on an Ethylenediamine tetraacetic acid (EDTA) tube for complete blood count (CBC), tumor masses were divided into two parts: the first part was saved in formalin 10% for histology and another part in Triazol for RNA extraction.

2.6. Molecular Analysis

The primer sequence for each gene is mentioned in Table (1). Thermal cycling conditions for *BAX* and *BCL2* gene were as follows, incubation at 42 ℃ for 20 minutes, Pre-denaturation, at 95 °C for 2 minutes, denaturation at 94 °C for 10 seconds and annealing , 60 °C for 40 seconds; 40 cycles [25]. The cycling condition for the *GAPDH* gene was 40 cycles with the following conditions: pre-denaturation at 95 ℃ for 30 s, denaturation at 95 °C for 10 s, and annealing at 60 °C for 30 s. The SYBR Green fluorescence signal was then continuously collected while the temperature was raised from 65 to 95 °C to create a melting curve [26]. The real-time polymerase chain reaction (RT-PCR) was performed on a Bio-Rad real-time PCR apparatus and thermal cyclers. The data was analyzed using CFX Manager software [27].

Table (1): The primer sequences of *GAPDH*, *BAX*, and *BCL2* and their codes at *NCBI*

Gene	*Primer set*	*Sequence*	*Reference*	*ID code at NCBI*
GAPDH	***Forward***	TGCCACTCAGAAGACTGTGG	***[26]***	NM_001394060.2
	Reverse	TTCAGCTCTGGGATGACCTT		
BAX	***Forward***	ACAGGGTTGAPDHTCATCCAGGATCGAG	***[25]***	NM_017059.2
	Reverse	AGCTCCATGTTGTTGTCCAGTTC		
BCL2	***Forward***	GGATTGTGGCCTTCTTTGAGTTC		NM_016993.2
	Reverse	AGAGCGATGTTGTCCACCAG		

2.1. Complete Blood Count (CBC)

The total blood count was evaluated using the CELL-DYN 1700 (Abbott Diagnostics, Abbott Park, IL, USA).

2.2. Statistical analysis methods

The study utilized IBM SPSS version 22.0 for Windows for statistical analysis, calculating mean, standard error, and P values. Data was analyzed using one-way ANOVA and Post Hoc LSD test, with P-values ≤0.05 indicating statistical significance and ≤0.01 indicating highly significant differences.

RESULTS

1. Transmission Electron Microscopy (TEM)

TEM is a powerful technique to investigate the shape and size of prepared nanoparticles. In this work, TEM was used to determine the shape and the size of SeNPs which were capped with AG to produce a core-shell structure (Se@AG). Figure (1) shows selenium nanoparticles surrounded with AG and the morphological shape is quasi-spherical. The size of Se@AG was determined to be in the range between (17.8 nm – 70.7 nm). Also, it is noticed that Se@AG nanostructure was homogenously distributed and no agglomerations were observed in the TEM image.

2. Survival rate:

The study found a significant difference in survival rate between the positive control group and the treated group using Kaplan-Meier analysis. There is a high significant difference between the two groups (*P*-value = 0.001) where the survival rate was recorded at 75% in the treated group compared to 20% in the positive control group as shown in Table (2) and Figure (2).

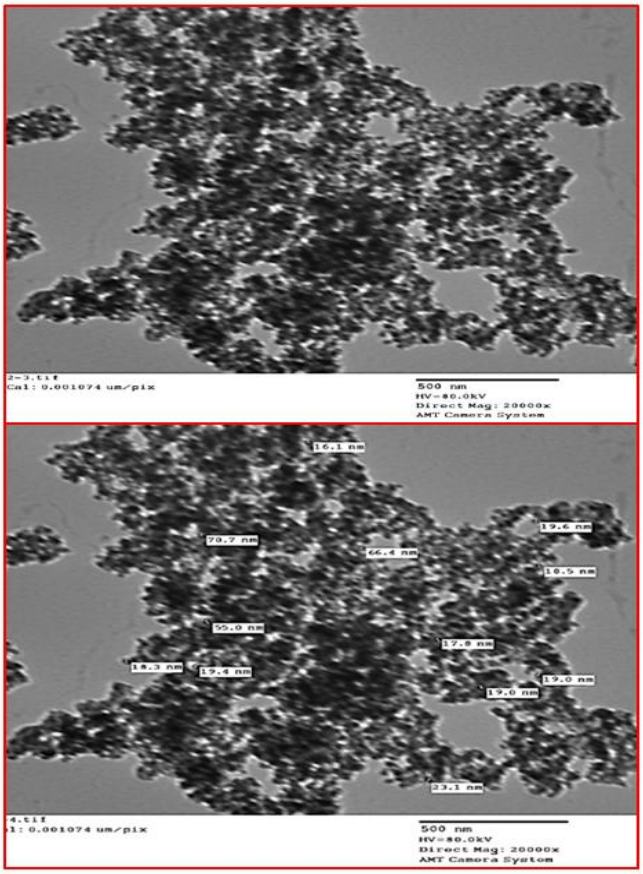

Fig. (1): TEM image shows the size range of Se@AG nanostructure (17.8 nm – 70.7 nm)

Table (2) shows the number of deaths and censored events and their percents in the three groups (negative control, positive control, and treatment):

Case Processing Summary					
Groups	Total No.	No. of Events (Deaths)		Censored	
		N	Percent	N	Percent
Negative Control	10	0	0%	10	100%
Positive Control	20	16	80%	4	20%
Treatment	20	5	25%	15	75%

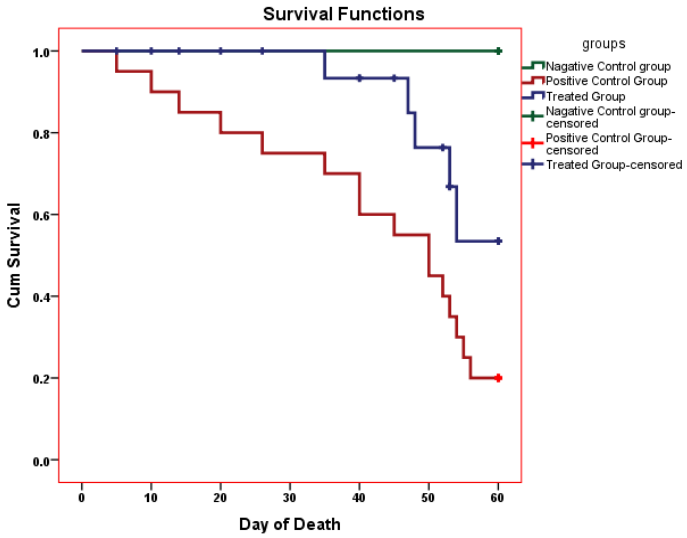

Fig. (2): Kaplan-Meier analysis for survival rate in positive control and treated groups showing the time of each event through experiment (20% and 75%, respectively)

3. Tumor volume

The tumor volume was measured by caliper at the time of starting treatment protocol and confirmed there is no significant difference between positive control and treated groups (*P*-value= 0.773) and they recorded 68.68±5.37 mm^3 and 71.42±7.79 mm^3, respectively. The treatment protocol continued for 8 weeks, reaching 161.8±23.32 mm^3 of tumor volume in the positive control group and the treated group and the size decreased to 9.98±0.93 mm^3. No significant difference in tumor volume between the two groups was observed until the 3rd week where the *P*-values recorded 0.59 and 0.26 in week (1) and week (2), respectively.

Table (3): The weekly recorded tumor volume means (mm^3) in positive control and treated groups from the time of starting treatment protocol to the end of the experiment:

Week No.	Positive Control (mm^3)		Treatment (mm^3)		*P*-value
	Mean	N	Mean	N	
Zero Time	68.67±5.37	20	71.42±7.79	20	0.773
week 1	72.86±5.54	19	67.86±7.40	20	0.5942
week 2	71.77±5.40	17	61.75±6.73	20	0.2648
week 3	75.52±6.01	16	44.00±5.43	20	0.0032
week 4	80.83±6.89	15	36.33±3.96	20	< 0.01
week 5	90.41±8.18	14	28.39±3.10	19	< 0.01
week 6	98.18±10.23	12	20.08±1.85	17	< 0.01
week 7	108.92±12.50	11	14.69±1.33	17	< 0.01
week 8	161.80±23.32	4	9.98±0.93	15	< 0.01

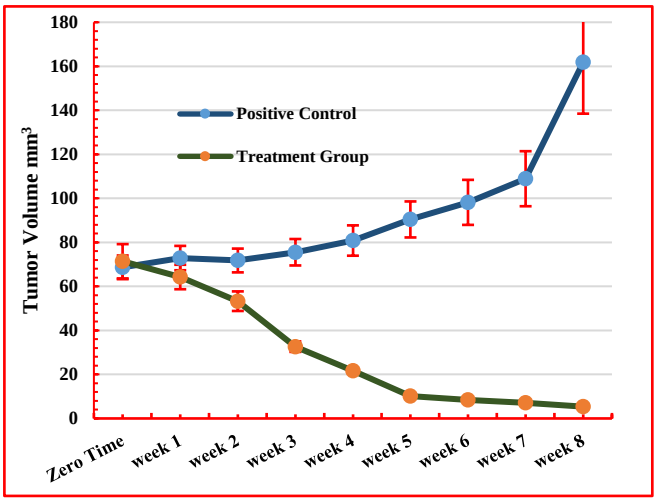

Fig. (3): Line graph showing the tumor volume changes through 8 weeks in positive control and treated groups with Se@Pt-AG-FA.

4. Histopathology

Hematoxylin and Eosin (H&E) examination of the negative control group revealed normal mammary glands and bland parenchymal stroma as shown in Figure (4A). However, H&E of the positive control group showed ductal neoplastic proliferation linked to the formation of invasive ductal carcinoma (IDC) of non-special type (NST) as shown in Figure (4B). Regarding the treated group, H&E illustrated that 20% of 15 rats showed a complete treatment response, including fibrosis, chronic inflammation, and congestion as shown in Figure (4C), but 80% of the treated group showed a partial treatment response, with extensive necrosis with viable tumor cells, exhibiting hyperchromasia and pleomorphism as shown in figure (4D).

5. Gene expression for *BAX* and *BCL2*

The real-time program was used to record the amplification and melting curves for the *BAX* and *BCL2* genes as mentioned in figure (5) and figure (6). The gene expression in the negative control, positive control, and treated groups, revealed that *BCL2* expression, an anti-apoptotic gene, was down-regulated in the positive control group, while the apoptotic gene *BAX* was increased in the treated group, resulting in a 0.036 *BAX/BCL2* ratio in the positive control group and 87.993 in the treated group as shown in table (4).

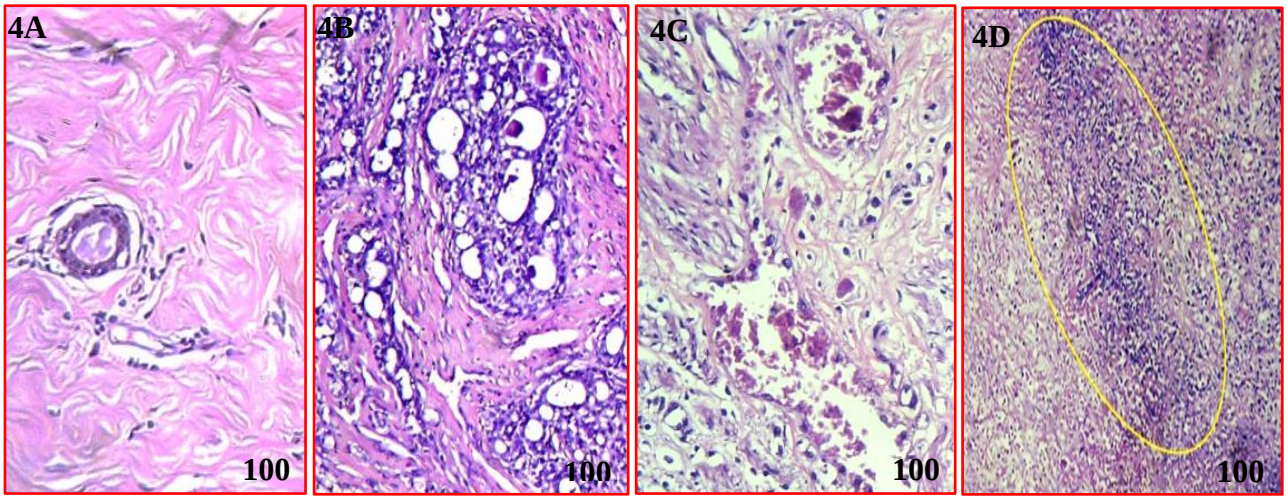

Fig. (4): H&E (100X) features of negative control, positive control, and treatment mammary gland in 4A, 4B, and 4C. 4A: acini forming small lobule and small duct surrounded by fibro-adipose tissue. 4B: IDC of NST is formed of mixed patterns including glandular structures, invasive cribriform nests, cords, and sheets in addition to identified necrosis. 4C: Skin is underlined by connective tissue showing congested blood vessels, fibrosis and inflammatory cellular infiltrate, and no residual malignant glands. 4D: The histologic appearance of breast carcinoma after therapy reveals a large amount of tumor necrosis together with a small number of remaining degraded tumor cells (yellow circle).

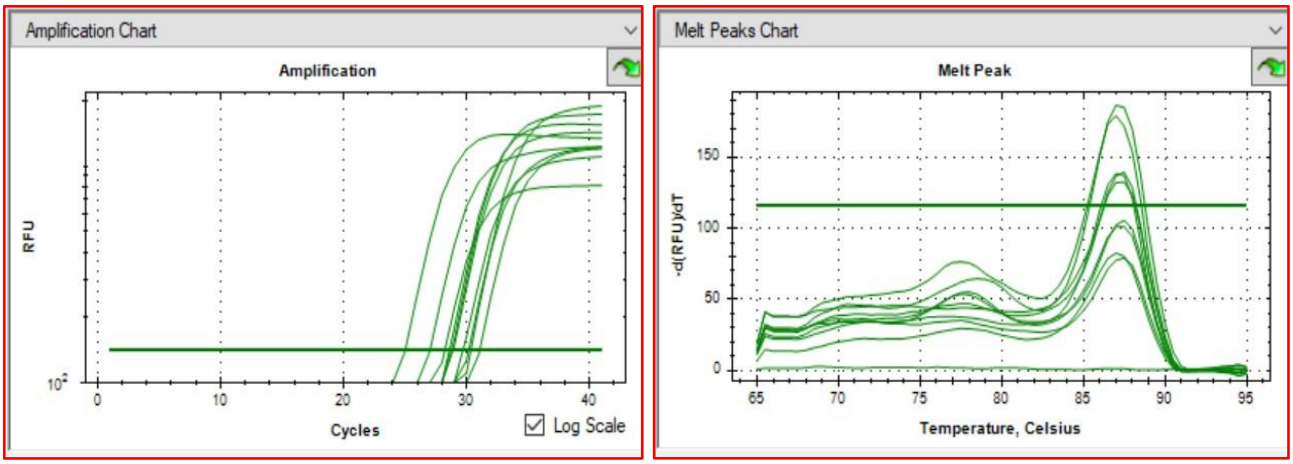

Fig. (5): Amplification and dissociation (Melting peak) curves for *BAX* gene expression

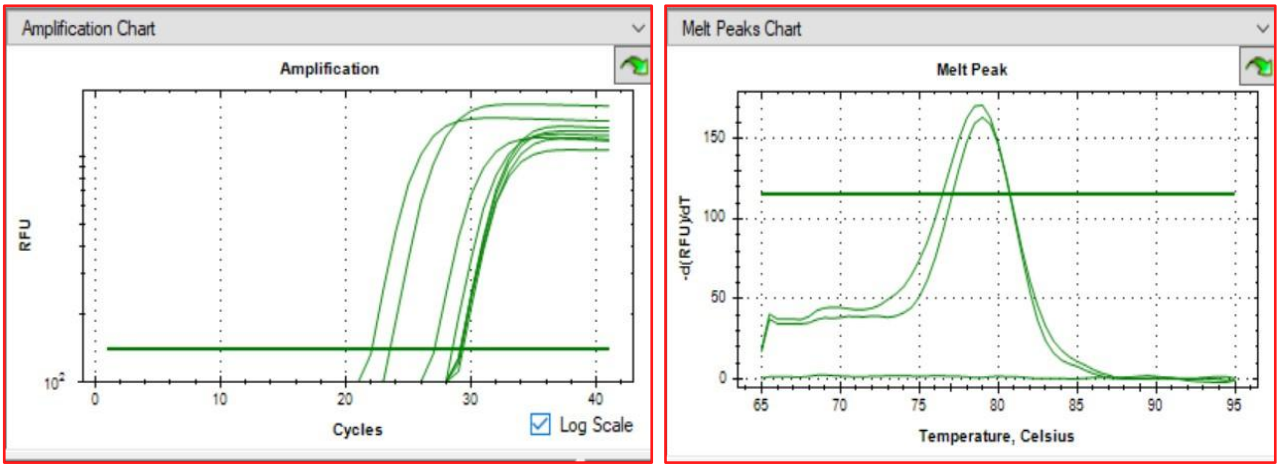

Fig. (6): Amplification and dissociation (Melting peak) curves for *BCl2* gene expression.

Table (4): shows *BAX* relative, *BCL2* relative, and *BAX/BCL2* ratio

Groups	*BAX*		*BCl2*		*BAX/BCl2* Ratio	Cell Status	
	BAX relative	Log *BAX*	*BCL2* relative	Log *BCL2*		Resistance	Apoptosis
Negative Control group	1	0	1	0	1		
Positive Control group	1.065	0.027	29.699	1.473	0.036	√	
Treated group	17.219	1.236	0.196	-0.708	87.993		√

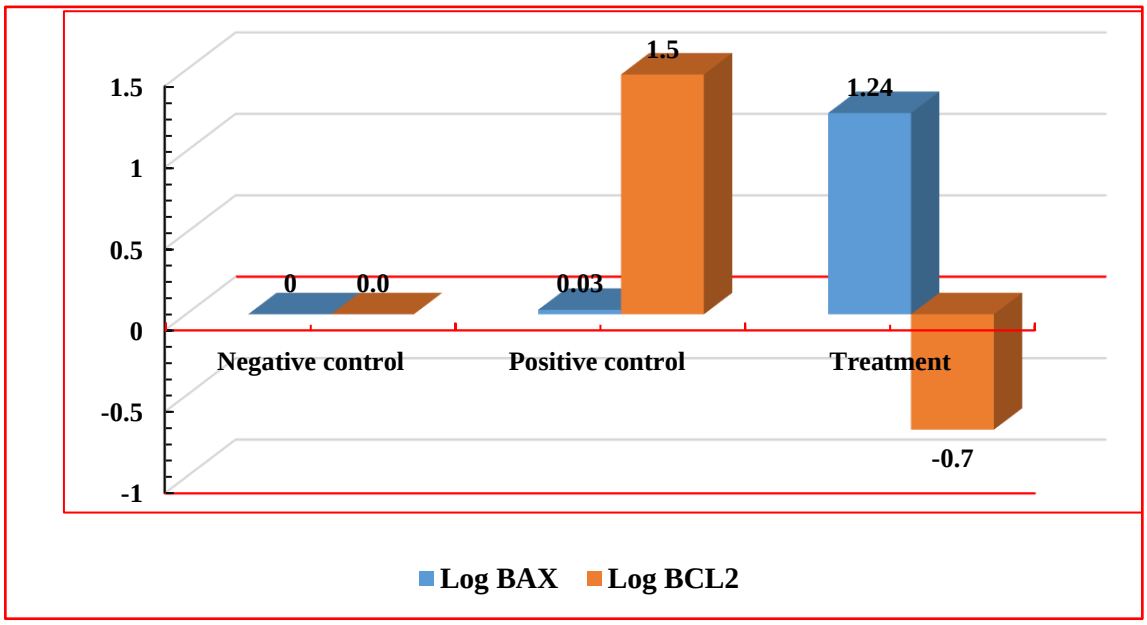

Fig. (7): The fold change in the expression of *BAX* and *BCL2* in the negative control, positive control, and treated groups.

6. Complete blood count (CBC)

In comparison to the positive control and negative control, there is a significant difference regarding the different hematological parameters including Haemoglobin (HGB), White Blood Cells (WBCs), Lymph % and Platelets (PLT), those changes represent some types of validation between positive control and negative control as a breast cancer model. Specifically, in comparison between the positive control and the treatment with Se@Pt-AG-FA recorded significant healing precursors where the HGB, lymph%, WBCs, and PLT recorded 25%, 114%, -60%, and -28%, respectively as a percent of change between two groups as showed in details in table (5).

Table (5): The means and *P-value*s versus normal and positive groups of the CBC parameters

CBC Parameters		WBC (10*9/L)	LYMPH (10*9/L)	MID (10*9/L)	Gran (10*9/L)	lymph%	Mid%	Gran%	RBC (10*12/L)	HGB (g/Dl)	HCT%	MCV (FI)	MCH (pg)	MCHC (g/Dl)	PLT (10*9/L)
Negative Control	Mean ± SEM	5.8±0.7^{a*}	3.2±1	0.6±0.12^{a*}	4.12±0.8^{a*}	49±5.5^{a}	8.5±2.2	49.2±6.4	7.1±0.2^{a*}	13.7±0.3^{a*}	43.5±0.9^{a*}	61.1±2.1^{a}	19.1±0.3^{a}	31.4±0.7	639.5±35.5^{a*}
Positive Control	Mean ± SEM	11.9±0.95^{b*}	5.9±0.3^{b}	0.1±0.001^{b*}	0.27±0.026^{b*}	22.2±1.3^{b}	12.9±1.04	41.2±3.29	5 ±0.23^{b*}	9.7±0.4^{b*}	35.4±3.1^{b*}	72.8±5.4^{b}	22±1^{b}	31.7±3	1069.5±93.8^{b*}
	% of change vs Normal	105%	82%	-83%	-93%	-55%	53%	-16%	-30%	-29%	-19%	19%	16%	1%	67%
Treatment	Mean ± SEM	4.8±0.4^{a*}	3.6±0.2	0.1±0.008^{b*}	0.8±0.048^{b*}	47.5±2.85^{a}	7.14±0.59	24.6±2.2^{b}	5.8±0.2^{b*}	12.2±0.13^{a*b*}	31±0.5^{b*}	52.5±2.9^{a*}	19.8±1.2	36.7±0.9^{ab}	775.2±40.7^{a}
	% of change vs Normal	-18%	13%	-80%	-81%	-3%	-16%	-50%	-19%	-11%	-29%	-14%	4%	17%	21%
	% of change vs +ve control	-60%	-38%	20%	196%	114%	-45%	-40%	15%	25%	-12%	-28%	-10%	16%	-28%

a: Significant difference vs Positive control (p-value< 0.05), a*: high significant difference vs Positive control (p-value<0.01), b: Significant difference vs Negative control (p-value< 0.05), b*: high significant difference vs Negative control (p-value< 0.01)

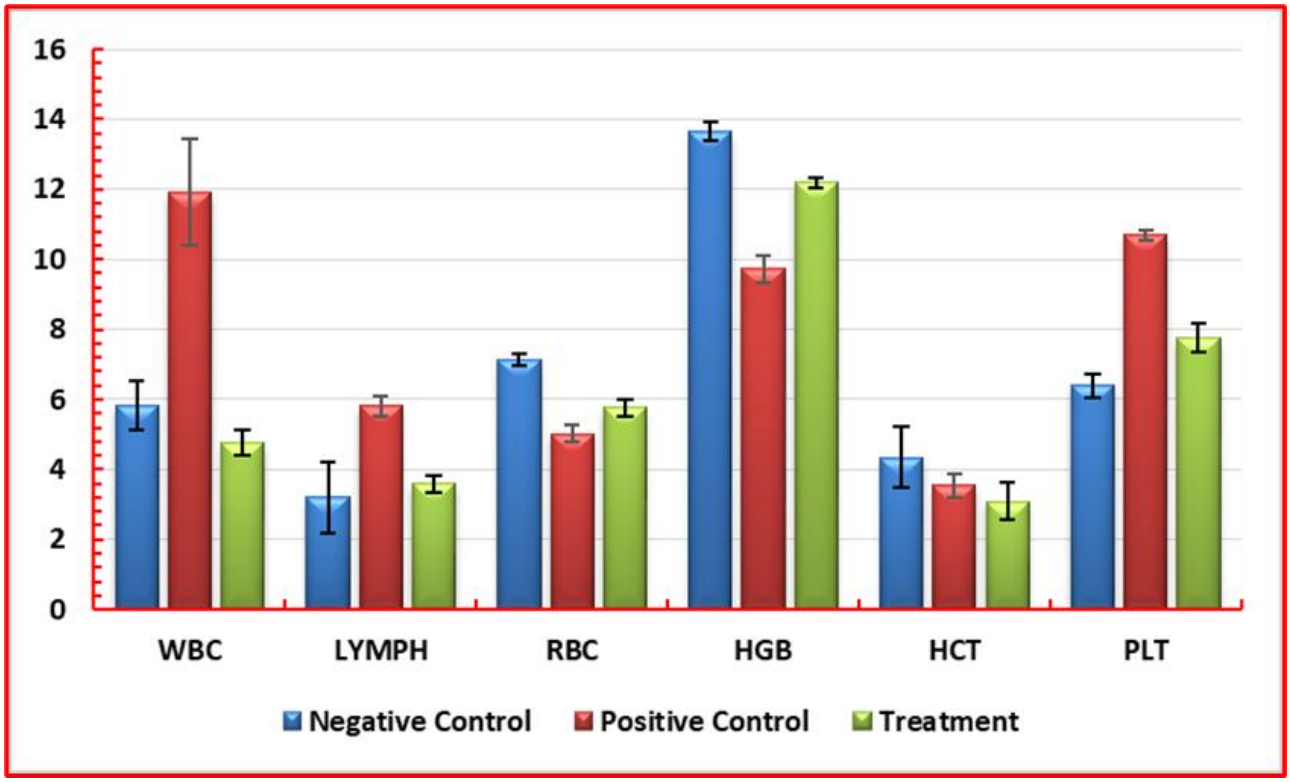

Fig. (8): shows the mean values of the CBC parameters in the negative control, positive control, and treated groups

DISCUSSION

Cancer, as an uncontrolled proliferation and dysfunctional disease, rapidly spreads worldwide without definite and fully safe treatment. Breast cancer incidence and its drawbacks have led to a higher mortality rate among cancer patients, with approximately 19 million new cases globally in 2020, resulting in 10 million deaths, according to the International Agency for Research on Cancer from the World Health Organization [1, 28]. Targeted therapy targets specific chemicals found in cancer cells to slow or stop tumor growth without damaging healthy cells through direct or indirect interaction. The study aims to develop a safe and efficient therapy for breast cancer patients using a new Nanoformula containing Pt, Se, AG, and FA, evaluates changes in the apoptotic pathways, and validates the results through H&E examination and toxicity assessment represented in blood cell analysis.

This study found that Se@Pt-AG-FA treatment significantly reduced tumor volume in the treated group by -86%, but increased it significantly in the positive control group by 126%, indicating the potentiality of Se@Pt-AG-FA in tumor shrinkage. [29]study found a 72% reduction in tumor volume using pterostilbene in TC-1 mice, and [30] study found a 50% reduction in tumor volume using *Pterocarpus Santalinus* containing Pt. Depending on the potentiality of Se@Pt-AG-FA on tumor reduction, the survival rate was improved significantly, saving 75% of animals compared to 25% in the positive control group.

The study found an upregulation of gene expression for *BAX* as an apoptotic marker in breast cancer animals and a downregulation of gene expression for *BCl2* as an anti-apoptotic marker. The current results agree with the finding of *Ramkumar's* review where Pt has been found to inhibit cell proliferation and induce apoptosis in certain cancerous cell lines by triggering intrinsic mitochondrial-derived apoptosis at the level of *in vitro* studies [8, 20]. At the level of *in vivo* study, Pt has been found to modify markers associated with mitochondrial apoptosis in prostate cancer models [31], increase pro-apoptotic markers in gastric adenocarcinoma cells [32], upregulate pro-apoptotic genes and anti-proliferative markers in pancreatic cancer [33], all of those results agree with our finding but do not agree with *Tang's* results where it inhibits apoptosis effects in vascular endothelial cells[34].

Se has been shown to have anticancer properties through various mechanisms, including cell apoptosis, restraint of cell multiplication, regulation of redox state, detoxification of cancer-causing agents, immune system stimulation, and inhibition of angiogenesis [35]. It can be internalized into malignancy cells through endocytosis, initiating cell demise through mitochondria-interceded apoptosis [36]. The mechanism of selenium action is mainly due to selective and substantial Se accumulation, causing a drastic elevation of reactive oxygen species (ROS) in cancer cells that damage DNA and induce apoptosis [37]. Small NPs are more efficient than larger ones, with low perceived toxicity on the normal cells and enhanced cytotoxicity on the cancer cells [38]. Se NPs can stimulate mitochondrial cell death through upregulation of p53 in cancer cells, followed by activating caspase-9 and *BAX* (apoptotic genes) in addition to downregulation of *BCL2* gene expression (Anti-apoptotic gene), depleting mitochondrial membrane potential, and inducing apoptosis [39, 40]. FA-Se NPs have higher anticancer effects on cancer cells due to their overexpression of folate receptors and enhanced ROS production in addition to the Mitochondrial cell death program [41].

At the level of prognosis, the *BAX/BCl2* ratio has a very critical role in determining the patient response to a specific treatment, for example, those finding of Helaly *et al* where found that the low *BAX/BCl2* ratio would make them an excellent marker for the *BCL2* inhibitory targeted chemotherapy to avoid resistance to the traditional therapy [42], the current results regarding to *BAX/BCl2* ratio it is recorded at about 88 which is an excellent indicator for a good prognosis whereas the result of this ratio in positive control for breast cancer recorded 0.04 as a bad prognosis in case of no treatment.

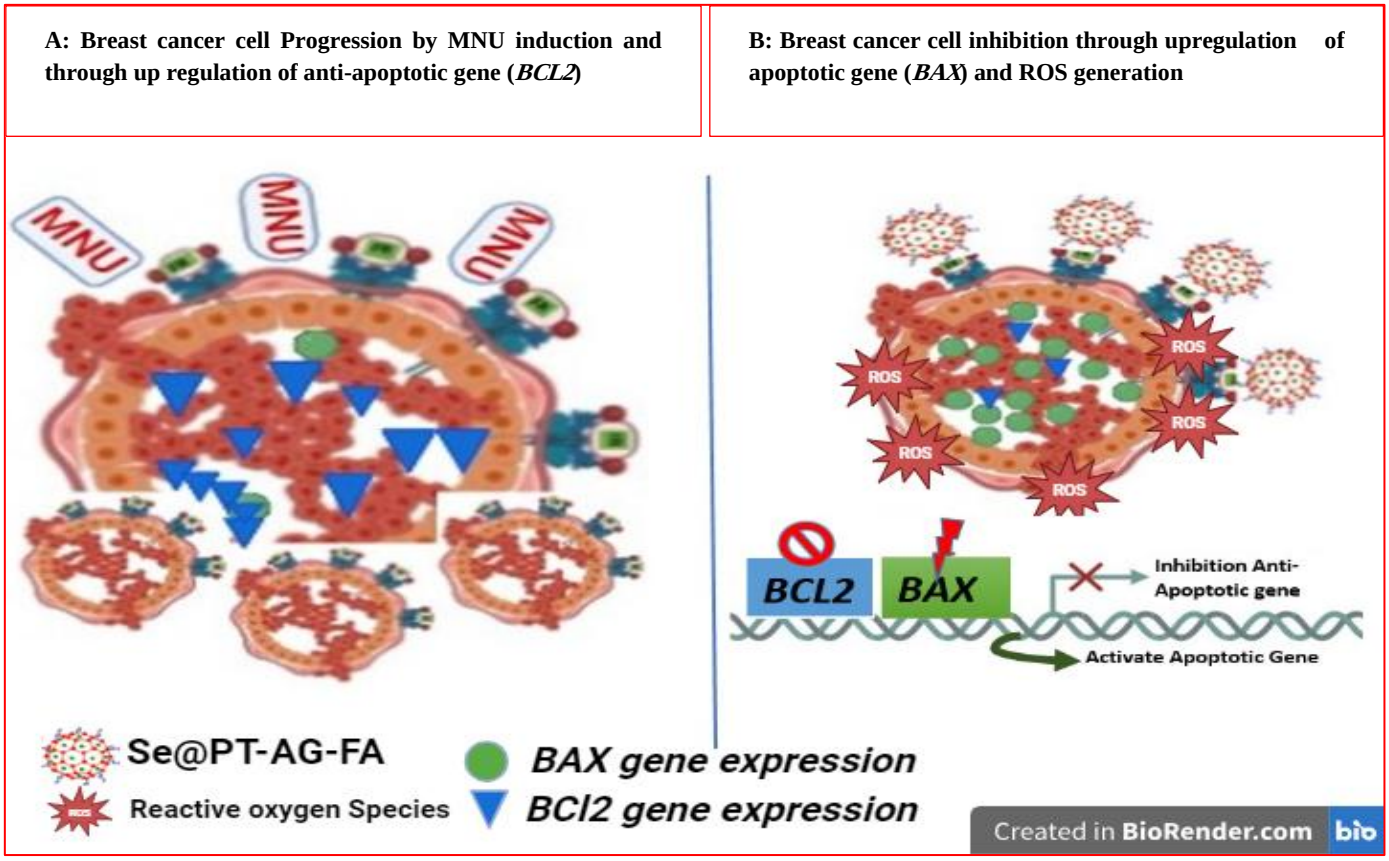

Fig. (9): A: showing the proliferation behavior of cancer cells under the activity of the Anti-apoptotic gene (*BCL2*) leading to cancer cell progression. B: Showing the prospected mechanism of action through molecular changes of apoptotic (*BAX*) and anti-apoptotic (*BCL2*) genes causing mitochondrial cell death in addition to increasing ROS production under the effect of the current nanoformulation (Se@Pt-AG-FA)

Histopathological findings show that MNU administration induces well-differentiated adenocarcinoma with various subtypes, including invasive cribriform nests, cords, and sheets with variable degrees of ductal epithelial reactions. MNU has been reported to induce carcinogenesis in various organs including mammary carcinomas which arise from MNU-induced hyperplastic alveolar nodules [43]. Through the interruption of the apoptotic pathway program caused by the MNU-induced cellular metabolic disruption, cell growth continued uncontrolled [44]. The study examined mammary glands and parenchymal stroma in rats with invasive ductal carcinoma. Hematoxylin and Eosin showed normal glands and bland parenchymal stroma in the negative control group. However, the positive control group showed ductal neoplastic proliferation, leading to invasive ductal carcinoma. 20% of the rats in the treated group showed complete treatment response, while 80% showed partial response with necrosis, tumor cells, hyperchromasia, and pleomorphism. Rats bearing breast tumors showed a significant suppression of tumor development with the Se@Pt-AG-FA nanoformulation therapy implying that the nanoformulation may be applied to the management of breast cancer.

The current research evaluates the hematological parameters of breast cancer induced in rats by MNU. The positive control group that bearing breast cancer recorded a significant decrease in some red blood cell parameters achieving anemic cases where the HGB, RBC count, and HCT recorded -29% (9.72±0.39), -30% (5.02±0.23), and -19% (35.37±3.14), respectively. The WBC and Lymph recorded a significant increase in percent change reaching 105% and 82% causing a severe type of inflammation. By the treatment, the current study found that the RBC count and hemoglobin were significantly increased in comparison to positive control recording percent change of 15% (5.76±0.24) and 25% (12.19±0.13), while the WBC and LYMPH were significantly decreased from positive control recording to -60% (4.76±0.35) and -38% (3.6±0.24). Also, our study finding regarding anemia agrees with the finding in the Indian study where 60% of breast cancer patients showed pretreatment anemia, which reduced after treatment [45]. Additional research revealed a significant decline in lymphocyte and total WBC counts from pre- to post-treatment. Treatments for breast cancer may be connected to the decrease in the WBC parameter [3]. The current results align with the Korean study that demonstrated treatment-induced reductions in WBC markers [45].

Regarding platelets, the treatment using Se@Pt-AG-FA restored the platelet count in the treated group (775.2±40.7) in comparison to the positive control (1069±93.8) recording -28% reduction in platelet count. The reason behind this might be the capacity of cancer cells to induce platelet aggregation and thrombocytosis [46]. According to the result of Mintesnot's study, there was an increase in thrombocytopenia before and after therapy [3]. Research has indicated that thrombocytopenia happens when breast cancer spreads, especially when it metastasizes to the bones. That is comparable to research done in Ethiopia that found thrombocytopenia to be prevalent there at a rate of 23.5% [47]. However, a study conducted in Switzerland revealed that thrombocytosis was increased throughout the treatment [48].

CONCLUSION

In conclusion, the current study showed that the radio-prepared Se@Pt-AG-FA nanoformulation contains Se NPs surrounded by AG, with a quasi-spherical morphology, and their size ranges from 17.8 nm – 70.7 nm. Also, the current findings demonstrated that Se@Pt-AG-FA enhances the survival rate which reaches 75% in the treated group, suppresses the breast tumor volume to reach 9.98±0.93 mm^3 versus 161.8±23.32 mm^3 in the positive control group, and gives 20% complete treatment response and 80% partial response through H&E examination. In addition, the analysis of gene expression in the treated group demonstrated a down-regulation of *BCL2* expression, but the apoptotic gene *BAX* was elevated, leading to the *BAX/BCL2* ratio reaching 87.993 as a significant indicator for the apoptosis effect of the current treatment. The study found significant differences in hematological parameters such as hemoglobin, white blood cells, lymph percentage, and platelets between a positive control and a negative control as a breast cancer model. Treatment with Se@Pt-AG-FA resulted in significant healing precursors, with HGB, lymph%, WBCs, and PLT showing significant changes between the two groups. Finally, Se@Pt-AG-FA shows a strong anticancer impact in models of breast cancer. So, expanding the validation studies on human cases as a targeted therapy for breast cancer is recommended.

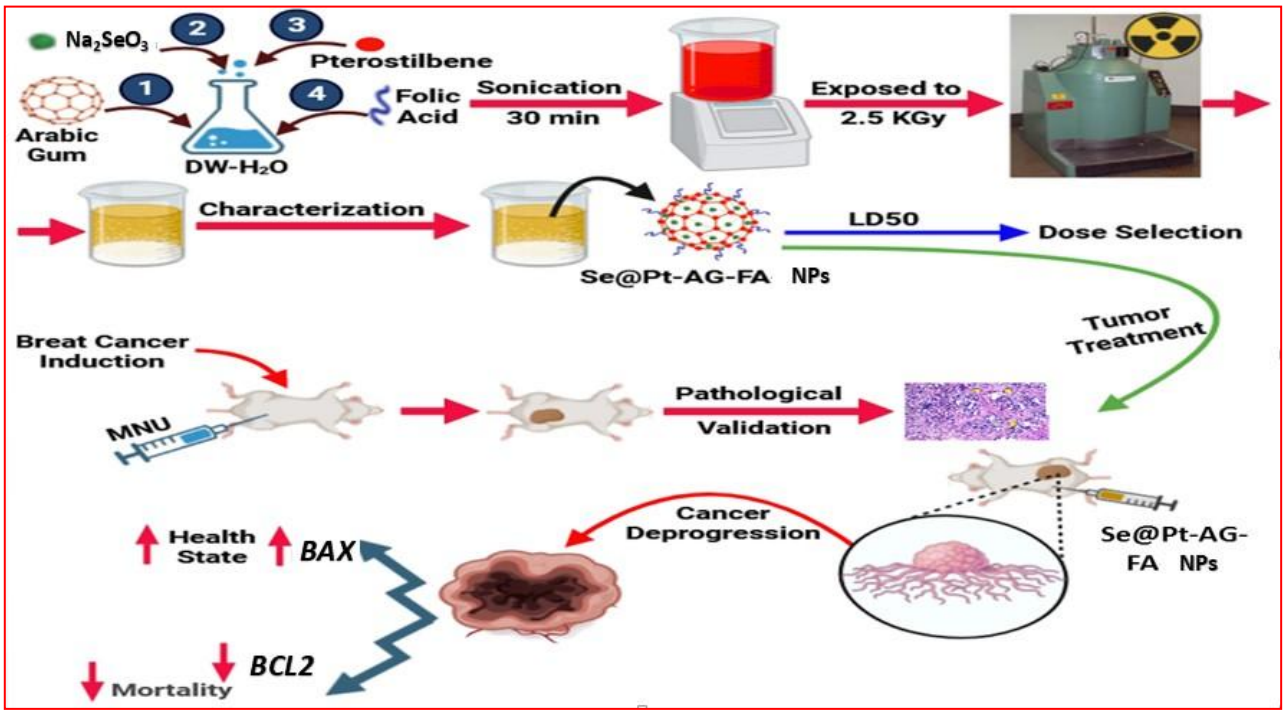

Fig. (10): showing graphical abstract of the current study. Se@Pt-AG-FA NPs nanoformulation is prepared by dissolving AG, Na_2SeO_3, Pt, and FA then sonicated and finally irradiated with 2.5 KGy. Characterization analysis confirmed the nanorange of the nanoformulation (17.8 nm – 70.7 nm). The breast cancer induction was performed by *in situ* injection of MNU (50 mg/kg). The nanoformulation was intraperitoneally applied to the tumor treatment in the MNU-breast cancer-bearing rats. Se@Pt-AG-FA NPs treatment (0.6 ml/rat = 4 mg/kg twice weekly for 2 months) showed tumor regression, upregulation of apoptotic gene expression (*BAX*), and downregulation of anti-apoptotic gene expression (*BCL2*).

Limitations

while Pterostilbene loaded on Arabic gum with folic acid and selenium in nanoformulations (Se@Pt-AG-FA) shows in the current study a promising effect in breast cancer treatment on animal models (Rats), these limitations highlight the challenges in translating preclinical results into effective human therapies. The limitations will be classified into main targets, the first regarding nano-characterization and validation which needed more tests such as Dynamic light scattering (DLS), zeta-potential, x-ray diffraction (XRD), and Scanning electron microscopy (SEM) imaging in addition to uptake and release assessment of the drug. The second target is regarding treatment evaluation and prognosis, some types of cachexia have appeared during treatment, so more examinations are needed as pyruvic transaminase (GPT), glutamic oxaloacetic transaminase (GOT), creatinine, Creatine kinase-MB (CK-MB), antioxidant activity, oxidative stress, microenvironments evaluations in addition to genetic studies related to cytogenetics and molecular biology.

REFERENCES

[1] Sung H, Ferlay J, Siegel RL, Laversanne M, Soerjomataram I, Jemal A, et al. Global cancer statistics 2020: GLOBOCAN estimates of incidence and mortality worldwide for 36 cancers in 185 countries. CA: a cancer journal for clinicians. 2021;71(3):209-49.

[2] Ramos A, Sadeghi S, Tabatabaeian H. Battling chemoresistance in cancer: root causes and strategies to uproot them. International journal of molecular sciences. 2021;22(17):9451.

[3] Min H-Y, Lee H-Y. Molecular targeted therapy for anticancer treatment. Experimental molecular medicine. 2022;54(10):1670-94.

[4] Carneiro BA, El-Deiry WS. Targeting apoptosis in cancer therapy. Nature reviews Clinical oncology. 2020;17(7):395-417.

[5] Maurya A, Singh AK, Mishra G, Kumari K, Rai A, Sharma B, et al. Strategic use of nanotechnology in drug targeting and its consequences on human

health: A focused review. Interventional Medicine Applied Science. 2019;11(1):38-54.

[6] Barchielli G, Capperucci A, Tanini D. The role of selenium in pathologies: an updated review. Antioxidants. 2022;11(2):251.

[7] Kim SJ, Choi MC, Park JM, Chung AS. Antitumor effects of selenium. International Journal of Molecular Sciences. 2021;22(21):11844.

[8] Nagarajan S, Mohandas S, Ganesan K, Xu B, Ramkumar KM. New insights into dietary pterostilbene: sources, metabolism, and health promotion effects. Molecules. 2022;27(19):6316.

[9] Liu P, Tang W, Xiang K, Li G. Pterostilbene in the treatment of inflammatory and oncological diseases. Frontiers in Pharmacology. 2024;14:1323377.

[10] Oršolić N, Jazvinšćak Jembrek M. Molecular and cellular mechanisms of propolis and its polyphenolic compounds against cancer. International journal of molecular sciences. 2022;23(18):10479.

[11] Surien O, Masre SF, Basri DF, Ghazali AR. Potential chemopreventive role of pterostilbene in its modulation of the apoptosis pathway. International Journal of Molecular Sciences. 2023;24(11):9707.

[12] Aloqbi AA. Gum Arabic as a natural product with antimicrobial and anticancer activities. Archives of pharmacy practice. 2020;11(2-2020):107-12.

[13] Ferro C, Florindo HF, Santos HA. Selenium nanoparticles for biomedical applications: from development and characterization to therapeutics. Advanced healthcare materials. 2021;10(16):2100598.

[14] Chaudhry G-e-S, Md Akim A, Sung YY, Sifzizul TMT. Cancer and apoptosis: The apoptotic activity of plant and marine natural products and their potential as targeted cancer therapeutics. Frontiers in Pharmacology. 2022;13:842376.

[15] Tagde P, Kulkarni GT, Mishra DK, Kesharwani P. Recent advances in folic acid engineered nanocarriers for treatment of breast cancer. Journal of Drug Delivery Science Technology. 2020;56:101613.

[16] Young O, Ngo N, Lin L, Stanbery L, Creeden JF, Hamouda D, et al. Folate receptor as a biomarker and therapeutic target in solid tumors. Current Problems in Cancer. 2023;47(1):100917.

[17] Singh R, Letai A, Sarosiek K. Regulation of apoptosis in health and disease: the balancing act of BCL-2 family proteins. Nature reviews Molecular cell biology. 2019;20(3):175-93.

[18] Abdel-Rafei MK, Askar MA, Azab KS, El-Sayyad GS, El Kodous MA, El Fatih NM, et al. FA-HA-Amygdalin@ Fe2O3 and/or γ-rays affecting SIRT1 regulation of YAP/TAZ-p53 signaling and modulates tumorigenicity of MDA-MB231 or MCF-7 cancer cells. Current Cancer Drug Targets. 2023;23(2):118-44.

[19] Askar MA, El-Sayyad GS, Guida MS, Khalifa E, Shabana ES, Abdelrahman IY. Amygdalin-folic acid-nanoparticles inhibit the proliferation of breast cancer and enhance the effect of radiotherapy through the modulation of tumor-promoting factors/immunosuppressive modulators in vitro. BMC Complementary Medicine Therapies. 2023;23(1):162.

[20] Thabet NM, Abdel-Rafei MK, El-Sayyad GS, Elkodous MA, Shaaban A, Du Y-C, et al. Multifunctional nanocomposites DDMplusAF inhibit the proliferation and enhance the radiotherapy of breast cancer cells via modulating tumor-promoting factors and metabolic reprogramming. Cancer Nanotechnology. 2022;13(1):16.

[21] Qian S, Wei Z, Yang W, Huang J, Yang Y, Wang J. The role of BCL-2 family proteins in regulating apoptosis and cancer therapy. Frontiers in oncology. 2022;12:985363.

[22] Liska J, Galbavy S, Macejova D, Zlatos J, Brtko J. Histopathology of mammary tumours in female rats treated with 1-methyl-1-nitrosourea. Endocrine regulations. 2000;34(2):91-6.

[23] Faustino-Rocha A, Oliveira PA, Pinho-Oliveira J, Teixeira-Guedes C, Soares-Maia R, Da Costa RG, et al. Estimation of rat mammary tumor volume using caliper and ultrasonography measurements. Lab animal. 2013;42(6):217-24.

[24] Abdelrahman IY, El-Kashef H, Hassan NH. Anti-tumor effect of green tea extract, simvastatin and gamma radiation on solid tumor in mice. Arab Journal of Nuclear Sciences Applications. 2020;53(4):39-52.

[25] Ramezani N, Vanaky B, Shakeri N, Soltanian Z, Rad FF, Shams Z. Evaluation of Bcl-2 and Bax Expression in the Heart of Diabetic Rats after Four

Weeks of High Intensity Interval Training. Medical Laboratory Journal. 2019;13(1).

[26] Zhang W-X, Fan J, Ma J, Rao Y-S, Zhang L, Yan Y-E. Selection of suitable reference genes for quantitative real-time PCR normalization in three types of rat adipose tissue. International journal of molecular sciences. 2016;17(6):968.

[27] Livak KJ, Schmittgen TD. Analysis of relative gene expression data using real-time quantitative PCR and the 2− ΔΔCT method. methods. 2001;25(4):402-8.

[28] Askar MA, El Shawi OE, Mansour NA, Hanafy AM. Breast cancer suppression by curcumin-naringenin-magnetic-nano-particles: In vitro and in vivo studies. Tumor Biology. 2021;43(1):225-47.

[29] Chatterjee K, Mukherjee S, Vanmanen J, Banerjee P, Fata JE. Dietary polyphenols, resveratrol and pterostilbene exhibit antitumor activity on an HPV E6-positive cervical cancer model: an in vitro and in vivo analysis. Frontiers in oncology. 2019;9:352.

[30] Akhouri V, Kumar A, Kumari M. Antitumour property of Pterocarpus santalinus Seeds against DMBA-induced breast cancer in rats. Breast cancer: basic clinical research. 2020;14:1178223420951193.

[31] Chakraborty A, Gupta N, Ghosh K, Roy P. In vitro evaluation of the cytotoxic, anti-proliferative and anti-oxidant properties of pterostilbene isolated from Pterocarpus marsupium. Toxicology in vitro. 2010;24(4):1215-28.

[32] Zhao T, Wang C, Huo X, He ML, Chen J. Pterostilbene enhances sorafenib's anticancer effects on gastric adenocarcinoma. Journal of Cellular Molecular Medicine. 2020;24(21):12525-36.

[33] Jiang C-H, Sun T-L, Xiang D-X, Wei S-S, Li W-Q. Anticancer activity and mechanism of xanthohumol: a prenylated flavonoid from hops (Humulus lupulus L.). Frontiers in pharmacology. 2018;9:530.

[34] Tang T, Duan Z, Xu J, Liang J, Zhang S, Zhang H, et al. Pterostilbene reduces endothelial cell injury in vascular arterial walls by regulating the Nrf2-mediated AMPK/STAT3 pathway in an atherosclerosis rat model. Experimental therapeutic medicine. 2020;19(1):45-52.

[35] Kuršvietienė L, Mongirdienė A, Bernatonienė J, Šulinskienė J, Stanevičienė I. Selenium anticancer properties and impact on cellular redox status. Antioxidants. 2020;9(1):80.

[36] Venugopal S. Therapeutic potential of selenium nanoparticles. Frontiers in Nanotechnology. 2022;4:1042338.

[37] Zhao G, Dong R, Teng J, Yang L, Liu T, Wu X, et al. N-Acetyl-l-cysteine enhances the effect of selenium nanoparticles on cancer cytotoxicity by increasing the production of selenium-induced reactive oxygen species. ACS omega. 2020;5(20):11710-20.

[38] Li C, Li Y, Li G, Wu S. Functional nanoparticles for enhanced cancer therapy. Pharmaceutics. 2022;14(8):1682.

[39] Hassan AA, Abdel-Rafei MK, Sherif NH, Askar MA, Thabet NM. Antitumor and radiosensitizing effects of Anagallis arvensis hydromethanolic extract on breast cancer cells through upregulating FOXO3, Let-7, and mir-421 Expression. Pharmacological Research-Modern Chinese Medicine. 2022;5:100179.

[40] Mikhailova EO. Selenium nanoparticles: green synthesis and biomedical application. Molecules. 2023;28(24):8125.

[41] Menon S, Ks SD, Santhiya R, Rajeshkumar S, Kumar V. Selenium nanoparticles: A potent chemotherapeutic agent and an elucidation of its mechanism. Colloids Surfaces B: Biointerfaces. 2018;170:280-92.

[42] Helaly NA, Esheba NE, Abou Ammo DE, Elwan NM, Elkholy RA. High Bax/Bcl-2 ratio is associated with good prognosis and better survival in patients with B cell chronic lymphocytic leukemia. Leukemia Research. 2021;107:106604.

[43] Gao D, Liu J, Yuan J, Wu J, Kuang X, Kong D, et al. Intraductal administration of N-methyl-N-nitrosourea as a novel rodent mammary tumor model. Annals of translational medicine. 2021;9(7).

[44] Askar MA, El-Nashar HA, Al-Azzawi MA, Rahman SSA, Elshawi OE. Synergistic effect of quercetin magnetite nanoparticles and targeted radiotherapy in treatment of breast cancer. Breast cancer: basic clinical research. 2022;16:11782234221086728.

[45] Macciò A, Madeddu C, Gramignano G, Mulas C, Tanca L, Cherchi MC, et al. The role of inflammation,

iron, and nutritional status in cancer-related anemia: results of a large, prospective, observational study. haematologica. 2015;100(1):124.

[46] Liu S, Fang J, Jiao D, Liu Z. Elevated platelet count predicts poor prognosis in breast cancer patients with supraclavicular lymph node metastasis. Cancer Management Research. 2020:6069-75.

[47] Hassen F, Enquoselassie F, Ali A, Addisse A, Taye G, Assefa M, et al. Socio-demographic and haematological determinants of breast cancer in a Tertiary Health Care and Teaching Hospital in Addis Ababa, Ethiopia. Ethiopian Journal of Health Development. 2021;35(2).

[48] Shilpa MD, Kalyani R, Sreeramulu P, Therapy. Prognostic value of pre-treatment routine hematological parameters in breast carcinoma: Advantageous or deleterious? Biomedical Research. 2020;7(8):3916-20.